# Experimental Investigation and Thermodynamic Calculation of Phase Equilibria in the Sn-Au-Ni System

X.J. LIU,[1,2] M. KINAKA,[1] Y. TAKAKU,[1] I. OHNUMA,[1,3] R. KAINUMA,[1] and K. ISHIDA[1]

1.—Department of Materials Science, Graduate School of Engineering, Tohoku University, Sendai 980-8579, Japan. 2.—Department of Materials Science and Engineering, Xiamen University, Xiamen 361005, P. R. China. 3. —Email: ohnuma@material.tohoku.ac.jp.

The phase equilibria of the Sn-Au-Ni system, including six isothermal section diagrams in the Sn-rich portion at 200–600°C, as well as three vertical sections at Au:Ni = 1:1, 50at.%Sn, and 40at.%Sn, were investigated by means of differential scanning calorimetry (DSC), x-ray diffraction, and metallography. The experimental results indicated that (1) there exists a ternary compound $Sn_4AuNi_2$ that is stable up to about 400°C, (2) there are larger solubilities of Au in the $Ni_3Sn_2$ phase in the Sn-Ni system and Ni in the SnAu phase in the Sn-Au system, and (3) there is the two-phase equilibrium between $Sn_2Ni_3$ and SnAu compounds below 400°C, rather than the continuous phase region from the $Sn_2Ni_3$ to the SnAu phases reported previously. Thermodynamic assessment of the Sn-Au-Ni system was also carried out by using the calculation of phase diagrams (CALPHAD) method, in which the Gibbs energies of the liquid, fcc, and hcp phases are described by the subregular solution model and that of compounds, including a ternary compound, are represented by the sublattice model. The thermodynamic parameters for describing each phase were optimized and good agreement between the calculated and experimental results was obtained.

**Key words:** Thermodynamics of phase diagram, Pb-free solders, electronic packaging, calculation of phase diagrams (CALPHAD) method

## INTRODUCTION

In recent years, great attention has been given to the development of Pb-free Sn-base solders for electronic interconnection materials used in electronic devices because of the health and environmental safety problems caused by conventional Pb-Sn solders. In order to realize an electronic package with Pb-free solders, the interfacial reaction between Pb-free solders and substrate is also important. Generally, in the common metallization scheme of ball grid array (BGA) microelectronic packaging, a Cu substrate coated by Ni and Au is jointed with Pb-free Sn base solder. The outermost Au-coated Cu substrate serves to protect the substrate from corrosion and oxidation, and the Ni-coated layer provides a diffusion barrier that inhibits detrimental growth of Cu-Sn intermetallics. Although some experimental investigations on the interfacial reaction between Sn-base solders

and Au/Ni/Cu metallization have been reported,[1–4] the phase equilibria in the Sn-Au-Ni ternary system have not been studied in detail, with the exception of the phase equilibria determined by Neumann et al.[5] and Anhock et al.[6] Figure 1 shows the isothermal section at 400°C presented by Neumann et al.,[5] where there is a homogenous range from the $Sn_2Ni_3$ phase in the Sn-Ni system to the SnAu phase in the Sn-Au system, and a ternary compound exists in the Sn-rich portion. However, the isothermal section at room temperature determined by Anhock et al.[6] indicated that a phase equilibrium exists between the $Sn_2Ni_3$ phase and SnAu phase with larger solubilities of the third elements, rather than the continuous solid solution as reported by Neumann et al.[5] Therefore, some uncertainties regarding the phase equilibria of this system remain.

Calculation of phase diagrams (CALPHAD) has been recognized to be an important tool in the design of materials because it significantly decreases the amount of required experimental work.[7] Recently, the
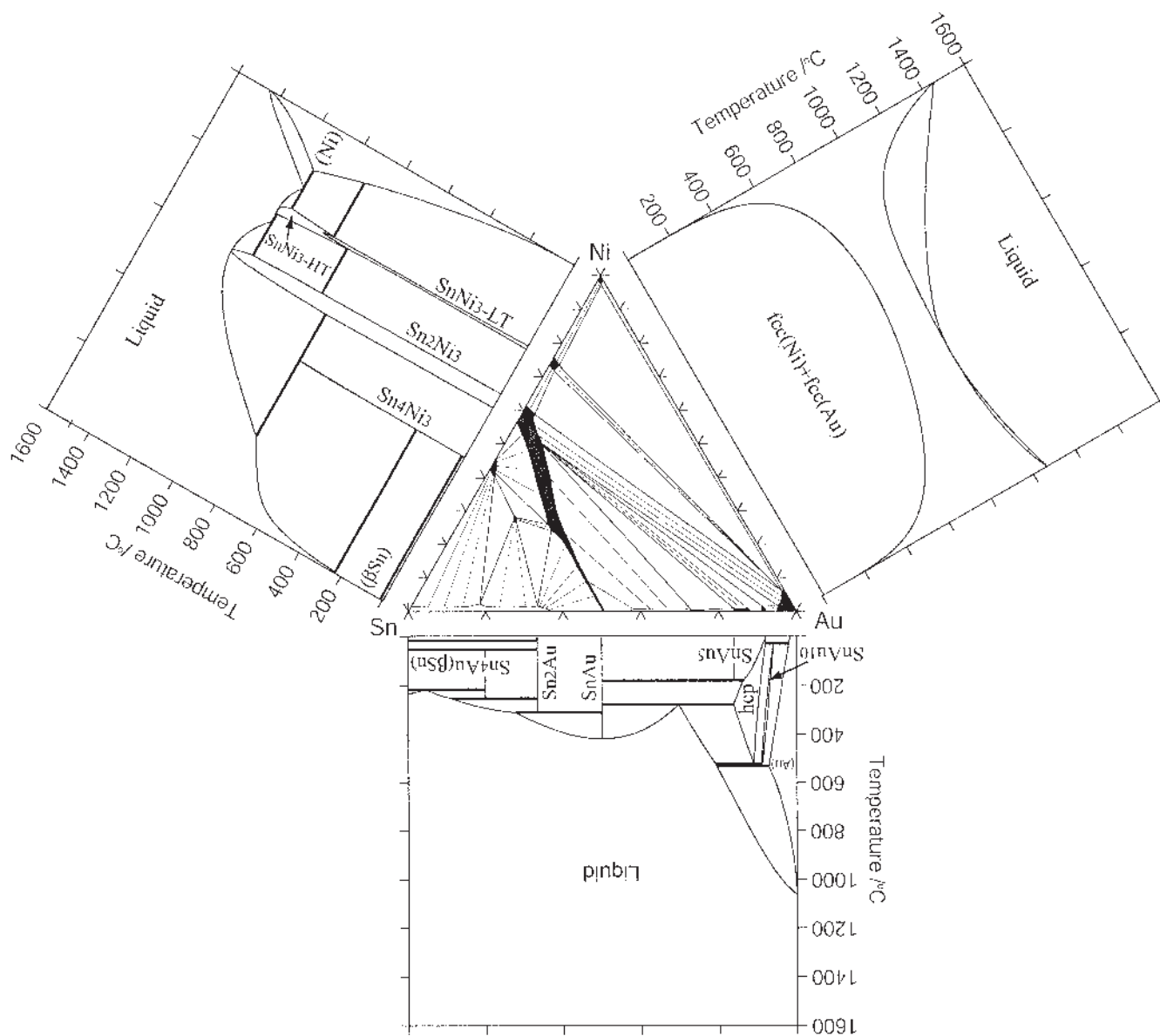
Fig. 1. Isothermal section at 400°C determined by Neumann et al.[5] and three sub-binary systems in the Sn-Au-Ni system.

present authors have developed a thermodynamic database for the design of solders in the framework of the CALPHAD method, which includes the elements Ag, Bi, Cu, In, Sn, Sb, Zn, and Pb, which can provide information on phase equilibria, liquidus projection, surface tension, and viscosity of the liquid phase, etc.[8–10] In order to understand the interfacial reactions between a substrate coated by Ni and Au and Pb-free solders, it is necessary to establish a thermodynamic database containing the elements of Au and Ni. The purpose of the present study was (1) to experimentally determine the phase equilibria in detail and (2) to carry out a thermodynamic assessment of the phase equilibria in the Sn-Au-Ni system.

## EXPERIMENTAL PROCEDURE

Sn-Au-Ni ternary alloys were prepared using pure Sn (99.9%), Au (99.99%), and Ni(99.9%) in evacuated transparent quartz capsules at about 1200°C for 4 h. After homogenization treatment, the specimens were equilibrated at 200°C, 250°C, 300°C, 400°C, 500°C, and 600°C for 20–720 h and then quenched in ice water. The quenched samples were cut and their surfaces were polished using $Al_2O_3$ powder. Equilibrium phase compositions in multiphase specimens were determined by a electron-probe microanalyzer (EPMA) using the standard calibration method. Transformation temperatures were determined by differential scanning calorimetry (DSC) using the heating curve. The experiments were carried out in a flowing argon atmosphere at rates of 3–10°C/min, using sintered $Al_2O_3$ as the reference specimen. X-ray diffraction was carried out using Cu $K_\alpha$ radiation to identify the crystal structure for the Sn-35Au-15Ni (at.%) and Sn-30Au-20Ni equilibrated at 300°C and 400°C for 40 days, respectively, in order to verify

**Table I. Information on the Crystal Structure and Modeling of Compounds in the Sn-Au-Ni System**

| Phase | Prototype | Pearson Symbol | Space Group | Struk-turbeicht Designation | Modeling | Ref. |
|---|---|---|---|---|---|---|
| SnAu | NiAs | hP4 | $P6_3/mmc$ | $B8_1$ | $Sn_{0.5}(Au,Ni)_{0.5}$ | 11 |
| $Sn_2Au$ | $AuSn_2$ | oP24 | Pbca | — | $Sn_{0.67}(Au,Ni)_{0.33}$ | 12 |
| $Sn_4Au$ | $PtSn_4$ | oC20 | Aba2 | $D1_c$ | $Sn_{0.8}(Au,Ni)_{0.2}$ | 13 |
| $SnAu_5$ | $Au_5Sn$ | hR6 | R3 | — | $Sn_{0.16}(Au,Ni)_{0.84}$ | 14 |
| $SnAu_{10}$ | $Ni_3Ti$ | hP16 | $P6_3/mmc$ | $D0_{24}$ | $(Au,Sn)$ | 12 |
| $SnNi_3$_HT | $Cu_3Ti$ | oP8 | Pmmm | — | $(Ni,Sn)_{0.25}(Ni,Sn)_{0.75}$ | 15 |
| $SnNi_3$_LT | $Ni_3Sn$ | hP8 | $P6_3/mmc$ | $D0_{19}$ | $(Ni,Sn)_{0.25}(Ni,Sn)_{0.75}$ | 16 |
| $Sn_2Ni_3$ | $InNi_2$ | hP6 | $P6_3/mmc$ | $B8_2$ | $(Ni,Sn)_{0.5}(Au,Ni)_{0.25}(Au,Ni)_{0.25}$ | 17 |
| $Sn_4Ni_3$ | CoGe | Mc16 | C2/m | — | $(Ni,Sn)_{0.5714}Ni_{0.4286}$ | 18 |
| $Sn_4AuNi_2$ | $Fe_3Sn_4$-s | — | R3m | — | $Sn_{0.571}Au_{0.143}Ni_{0.286}$ | 19 |

whether there exits a continuous solid solution from the $Sn_2Ni_3$ phase to the SnAu phase as reported by Neumann et al.[5]

## THERMODYNAMIC MODELS

The crystal structures of the compounds in the Sn-Au-Ni ternary system are listed in Table I.[11–19] The Gibbs energy of each phase is described as follows.

### Solution Phases

The Gibbs energies of solution phases, such as the liquid, fcc, hcp, and βSn phases in the Sn-Au-Ni system, are described by the subregular solution model with the Redlich–Kister formula[20] as follows:

$$G_m^\phi = \sum_{i=Au,Ni,Sn} {}^0G_i^\phi x_i^\phi + RT \sum_{i=Au,Ni,Sn} x_i^\phi \ln x_i^\phi$$
$$+ x_{Au}^\phi x_{Ni}^\phi L_{Au,Ni}^\phi + x_{Au}^\phi x_{Sn}^\phi L_{Au,Sn}^\phi$$
$$+ x_{Ni}^\phi x_{Sn}^\phi L_{Ni,Sn}^\phi + \Delta^{ex}G^{tern}$$

where ${}^0G_i^\phi$ denotes the molar Gibbs energy of the pure component i with $\phi$ phase, $x_i$ is the mole fraction of component i, R is the gas constant, and T is the absolute temperature. The term $L_{i,j}^\phi$ is the interaction parameter between i and j atoms in the i-j binary system, and $\Delta^{ex}G^{tern}$ is the excess term of the interaction between atoms in the ternary system, which can be expressed in the following forms, respectively:

$$L_{i,j}^\phi = \sum_{m=0}^n {}^mL_{i,j}^\phi \left(x_i - x_j\right)^m$$

$$\Delta^{ex}G^{tern} = x_{Au}^\phi x_{Ni}^\phi x_{Sn}^\phi \left( x_{Au}^\phi \, {}^0L_{AuNiSn}^\phi + x_{Ni}^\phi \, {}^1L_{AuNiSn}^\phi \right.$$
$$\left. + x_{Sn}^\phi \, {}^2L_{AuNiSn}^\phi \right)$$

where the coefficient ${}^mL_{i,j}^\phi$ represents the parameters in the sub-binary system, and ${}^nL_{AuNiSn}^\phi$ may be temperature dependent and is optimized in the present calculation.

### Compound Phases

(a) The solubilities of the third element in the $Sn_2Au$, $SnAu_{10}$, and $SnAu_5$ phases in the Sn-Au system and the $SnNi_3$, $Sn_2Ni_3$, and $Sn_4Ni_3$ phases in the Sn-Ni system are ignored, and the description of Gibbs energies of these phases is the same as those in the binary system.

(b) The Gibbs energies of the $Sn_4Au$ and SnAu phases with the solubility of the Ni element are described by the two sublattices,[21] i.e., $Sn_{0.8}(Au,Ni)_{0.2}$ and $Sn_{0.5}(Au,Ni)_{0.5}$. Their Gibbs energies are, respectively, expressed by

$$G^{Sn_4Au} = y_{Au}^{II} \, {}^0G_{Sn:Au} + y_{Ni}^{II} \, {}^0G_{Sn:Ni} + 0.2RT$$
$$\left(y_{Au}^{II} \ln y_{Au}^{II} + y_{Ni}^{II} \ln y_{Ni}^{II}\right) + y_{Au}^{II} y_{Ni}^{II} L_{Sn:Au,Ni}$$

$$G^{SnAu} = y_{Au}^{II} \, {}^0G_{Sn:Au} + y_{Ni}^{II} \, {}^0G_{Sn:Ni} + 0.5RT$$
$$\left(y_{Au}^{II} \ln y_{Au}^{II} + y_{Ni}^{II} \ln y_{Ni}^{II}\right) + y_{Au}^{II} y_{Ni}^{II} L_{Sn:Au,Ni}$$

where $y_i^{II}$ is the fraction of element i in sublattice II and ${}^0G_{i:j}$ is the Gibbs energy of formation of the compound ij. The L term is the interaction parameter between Au and Ni in sublattce II.

(c) Since there is a larger solubility of Au in the $Sn_2Ni_3$ phase in the Ni-Sn system, its Gibbs energy is described by three sublattices, i.e., $(Ni,Sn)_{0.5}(Au,Ni)_{0.25}(Au,Ni)_{0.25}$, as follows:

$$G = y_{Ni}^I y_{Au}^{II} y_{Au}^{III} \, {}^0G_{Ni:Au:Au} + y_{Ni}^I y_{Au}^{II} y_{Ni}^{III} \, {}^0G_{Ni:Au:Ni}$$
$$+ y_{Ni}^I y_{Ni}^{II} y_{Au}^{III} \, {}^0G_{Ni:Ni:Au} + y_{Ni}^I y_{Ni}^{II} y_{Ni}^{III} \, {}^0G_{Ni:Ni:Ni}$$
$$+ y_{Sn}^I y_{Au}^{II} y_{Au}^{III} \, {}^0G_{Sn:Au:Au} + y_{Sn}^I y_{Au}^{II} y_{Ni}^{III} \, {}^0G_{Sn:Au:Ni}$$
$$+ y_{Sn}^I y_{Ni}^{II} y_{Au}^{III} \, {}^0G_{Sn:Ni:Au} + y_{Sn}^I y_{Ni}^{II} y_{Ni}^{III} \, {}^0G_{Sn:Ni:Ni}$$
$$+ 0.5RT\left(y_{Ni}^I \ln y_{Ni}^I + y_{Sn}^I \ln y_{Sn}^I\right) + 0.25RT$$
$$\left(y_{Au}^{II} \ln y_{Au}^{II} + y_{Ni}^{II} \ln y_{Ni}^{II}\right) + 0.25RT\left(y_{Au}^{III} \ln y_{Au}^{III}\right.$$
$$\left. + y_{Ni}^{III} \ln y_{Ni}^{III}\right) + y_{Ni}^I y_{Sn}^I \left(y_{Au}^{II} y_{Au}^{III} L_{Ni,Sn:Au:Au}\right.$$
$$+ y_{Au}^{II} y_{Ni}^{III} L_{Ni,Sn:Au:Ni} + y_{Ni}^{II} y_{Au}^{III} L_{Ni,Sn:Ni:Au}$$
$$\left. + y_{Ni}^{II} y_{Ni}^{III} L_{Ni,Sn:Ni:Ni}\right) + y_{Au}^{II} y_{Ni}^{II} \left(y_{Ni}^I y_{Au}^{III} L_{Ni:Au,Ni:Au}\right.$$
$$+ y_{Ni}^I y_{Ni}^{III} L_{Ni:Au,Ni:Ni} + y_{Sn}^I y_{Au}^{III} L_{Sn:Au,Ni:Au}$$
$$\left. + y_{Sn}^I y_{Ni}^{III} L_{Sn:Au,Ni:Ni}\right) + y_{Au}^{III} y_{Ni}^{III}$$
$$\left(y_{Ni}^I y_{Au}^{II} L_{Ni:Au:Au,Ni} + y_{Ni}^I y_{Ni}^{II} L_{Ni:Ni:Au,Ni}\right.$$
$$\left. + y_{Sn}^I y_{Au}^{II} L_{Sn:Au:Au,Ni} + y_{Sn}^I y_{Ni}^{II} L_{Sn:Ni:Au,Ni}\right)$$

where $y_i^s$ is the fraction of element i in sublattice s, and $^0G_{i:j:k}$ is the Gibbs energy of formation of the compound ijk. The L term is the interaction parameter in the sublattices I, II, and III, respectively.

(d) The $Sn_4AuNi_2$ ternary compound is described as $Sn_{0.571}Au_{0.143}Ni_{0.286}$, and its Gibbs energy can be written as

$$G - 0.571 \, {}^0G_{Sn}^{bct} - 0.143 \, {}^0G_{Au}^{fcc} - 0.286 \, {}^0G_{Ni}^{fcc} = A + BT$$

where the parameters A and B are optimized based on the experimental data.

The unary data for the pure elements are taken from Dinsdale.[22]

## RESULTS AND DISCUSSION

### Determination of Phase Equilibria

Typical two- and three-phase microstructures of the Sn-12.5at.%Au-12.5at.%Ni and Sn-14at.%Au-29at.%Ni alloys equilibrated at 300°C and 500°C are shown in Fig. 2a and b, respectively. It is seen that a dendrite microstructure is formed from the liquid phase during cooling. The equilibrium compositions at the Sn-rich portion in the temperature range from 200°C to 600°C determined by EPMA are listed in Table II and presented in Fig. 3. The experimental results indicate that the phase equilibria in this system have the following features: (1) there is a ternary compound ($Sn_4AuNi_2$) in the Sn-rich portion, (2) there is the phase equilibrium between the $Ni_3Sn_2$ and the SnAu phases, and (3) there is a larger solubility of Ni in the $Sn_4Au$ phase in the Sn-Au system. Neumann et al. studied the crystal structure of the $Sn_4AuNi_2$ compound, and reported that it is stable up to 420°C, at which temperature it undergoes the peritectic reaction (L+ $Sn_4Ni_3$+ $Sn_2Ni_3$ ↔ $Sn_4AuNi_2$).[19] The present DSC results show that this peritectic reaction occurs at 422°C, which is in good agreement with the data reported by Neumann et al.[19] Neumann et al.[5] also

reported that there is a continuous solid solution from the $Ni_3Sn_2$ phase in the Sn-Ni system to the SnAu phase in the Sn-Au system. However, the present results indicate that there is a two-phase equilibrium between the SnAu and the $Sn_2Ni_3$ phases with a larger solubility of Ni and Au, respectively. In order to clarify this difference between the present findings and Neumann's results, x-ray diffraction was carried out for the Sn-35at.%Au-15at.%Ni and Sn-30at.%Au-20at.%Ni alloys. Figure 4 shows the patterns of x-ray diffraction and the corresponding microstructures, where the $SnAu_{35}Ni_{15}$ and $SnAu_{30}Ni_{20}$ alloys have single- and two-phase microstructures, respectively. It is seen that the x-ray pattern for the $SnAu_{35}Ni_{15}$ alloy shows a NiAs-type structure (Fig. 4a), while that for the $SnAu_{30}Ni_{20}$ alloy shows different structures between the SnAu and $Sn_2Ni_3$ phases (Fig. 4c). Fjellvag and Kjekshus reported that the $Sn_2Ni_3$ phase has a $Ni_2In$-type structure, rather than a full NiAs-type structure.[17] The present results indicate that the $Sn_4Au$ compound can dissolve up to 10.5at.%Ni at 200°C, which is in good agreement with findings reported by Song et al.[3] and Anhock et al.[6]

Vertical sections at 40at.%Sn, 50at.%Sn, and Au:Ni = 1:1 were also determined by DSC. These results are listed in Table III.

### Optimization of Phase Equilibria

The phase diagrams of the Sn-Ni, Sn-Au, and Ni-Au binary systems were thermodynamically assessed by Ghosh,[23] Liu et al.,[24] Morioka, and Hasebe,[25] respectively. Thermodynamic parameters in Refs. 24 and 25 were used in the present assessments. The parameters in the Sn-Ni system were mainly taken from Ghosh's assessment,[23] except for those of the $Sn_2Ni_3$ phase because the model describing this phase cannot reproduce the present experimental data. The optimized thermodynamic parameters for calculating the phase equilibria of
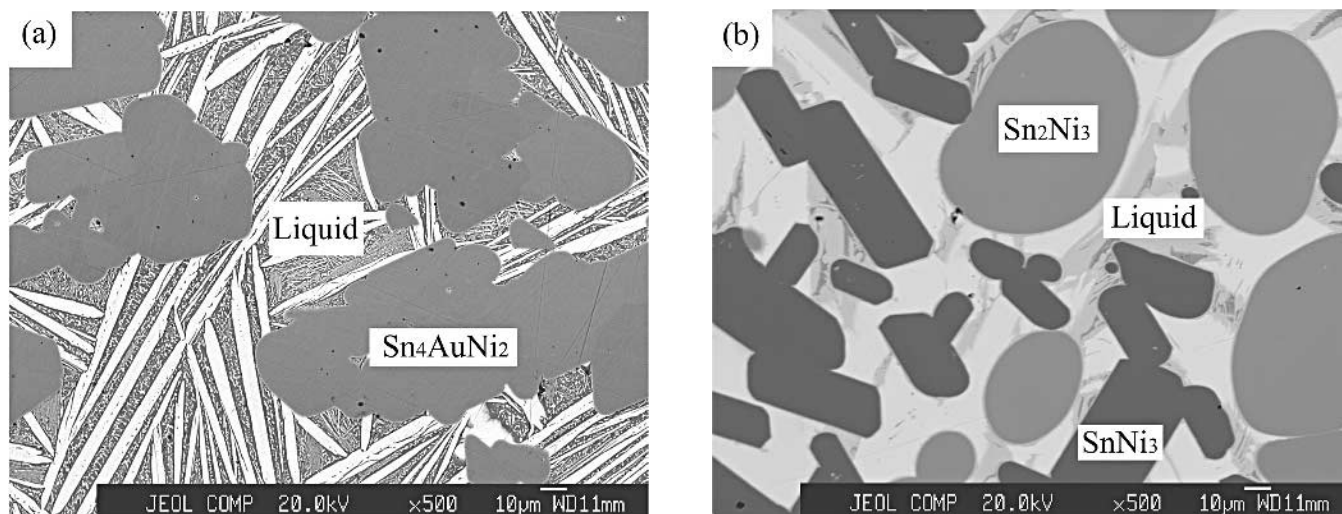


Fig. 2. Microstructures of (a) Sn-12.5at.%Au-12.5at.%Ni alloy treated at 300°C for 30 days and (b) Sn-14at.%Au-29at.%Ni alloy treated at 500°C for 20 h.

**Table II.  Phase Equilibrium Compositions of the Sn-Au-Ni System Determined By the Present Work**

| Temperature (°C) | Equilibria | Composition (At.%) | | | | | |
| --- | --- | --- | --- | --- | --- | --- | --- |
| | | Phase 1 | | Phase 2 | | Phase 3 | |
| | | Ni | Au | Ni | Au | Ni | Au |
| 600 | $Sn_2Ni_3$/liquid | 41.4 | 13.3 | 1.7 | 39.6 | — | — |
| | | 48.5 | 6.1 | 1.6 | 22.0 | — | — |
| | | 43.4 | 11.0 | 0.8 | 33.5 | — | — |
| | | 48.8 | 5.9 | 0.8 | 23.6 | — | — |
| | | 40.9 | 13.9 | 0.9 | 45.7 | — | — |
| | | 50.4 | 8.3 | 2.0 | 68.4 | — | — |
| | | 46.4 | 10.8 | 2.0 | 62.2 | — | — |
| | | 45.3 | 11.6 | 2.9 | 56.4 | — | — |
| | $SnNi_3$/liquid | 44.7 | 0.2 | 1.8 | 15.1 | — | — |
| | | 45.0 | 0.18 | 2.7 | 17.7 | — | — |
| 500 | $Sn_2Ni_3$/liquid | 31.4 | 19.9 | 1.2 | 34.3 | — | — |
| | | 28.8 | 23.5 | 0.5 | 46.5 | — | — |
| | | 48.5 | 9.5 | 1.5 | 70.2 | — | — |
| | | 43.9 | 13.1 | 1.2 | 64.7 | — | — |
| | | 39.9 | 16.0 | 0.7 | 62.4 | — | — |
| | $SnNi_3$/liquid | 44.2 | 0.5 | 0.6 | 25.0 | — | — |
| | | 43.1 | 0.3 | 1.7 | 16.0 | — | — |
| | | 43.3 | 0.4 | 1.0 | 19.3 | — | — |
| | $Sn_2Ni_3$/$SnNi_3$/liquid | 44.1 | 0.5 | 41.3 | 11.6 | 1.2 | 24.8 |
| 500 | $Sn_2Ni_3$/$SnNi_3$/liquid | 43.6 | 0.5 | 40.6 | 11.9 | 0.9 | 25.0 |
| 400 | $Sn_2Ni_3$/liquid | 21.6 | 25.9 | 0.3 | 31.4 | — | — |
| | | 40.4 | 16.2 | 0.9 | 68.1 | — | — |
| | | 30.0 | 23.9 | 0.6 | 55.5 | — | — |
| | $SnNi_3$/liquid | 42.2 | 0.8 | 1.0 | 16.4 | — | — |
| | | 42.0 | 0.9 | 0.7 | 20.1 | — | — |
| | $Sn_4AuNi_2$/liquid | 28.9 | 13.6 | 0.7 | 21.1 | — | — |
| | $Sn_2Ni_3$/$SnNi_3$ | 37.1 | 14.8 | 43.1 | 0.5 | — | — |
| | $Sn_2Ni_3$/hcp | 46.8 | 11.3 | 1.7 | 86.3 | — | — |
| | $SnAu$/$Sn_2Ni_3$ | 18.0 | 31.9 | 22.6 | 26.8 | — | — |
| 300 | $Sn_4AuNi_2$/liquid | 28.4 | 13.5 | 0.4 | 10.4 | — | — |
| | $Sn_2Ni_3$/$SnNi_3$ | 44.4 | 9.8 | 44.0 | 0.8 | — | — |
| | $Sn_2Ni_3$/hcp | 34.2 | 20.4 | 1.6 | 83.9 | — | — |
| | | 49.2 | 9.8 | 84.3 | 2.0 | — | — |
| | $SnAu$/$Sn_2Ni_3$ | 17.7 | 32.2 | 23.5 | 26.1 | — | — |
| | $Sn_4AuNi_2$/$SnNi_3$/liquid | 28.3 | 13.6 | 20.7 | 25.5 | 0.2 | 20.8 |
| | $Sn_4AuNi_2$/$SnAu$/liquid | 28.6 | 13.5 | 41.7 | 0.7 | 0.8 | 9.0 |
| | $Sn_3Ni_2$/hcp/liquid | 22.9 | 29.2 | 0.1 | 83.1 | 0.2 | 69.7 |
| | $Sn_2Ni_3$/$SnAu$/hcp | 17.7 | 27.8 | 10.9 | 35.3 | 0.6 | 31.9 |
| 250 | $Sn_4AuNi_2$/liquid | 28.9 | 13.5 | 0.6 | 11.3 | — | — |
| | $SnNi_3$/liquid | 42.7 | 0.3 | 0.5 | 4.8 | — | — |
| | $Sn_4AuNi_2$/$Sn_2Au$/liquid | 28.9 | 13.6 | 0.5 | 31.7 | 2.4 | 16.8 |
| 200 | $Sn_4AuNi_2$/$Sn_4Au$ | 28.1 | 13.6 | 7.6 | 11.6 | — | — |
| | $Sn_4Au$/βSn | 10.0 | 9.3 | 0.0 | 0.1 | — | — |
| | $SnNi_3$/$Sn_2Ni_3$ | 44.0 | 0.6 | 39.4 | 13.7 | — | — |
| | $Sn_2Ni_3$/hcp | 49.5 | 9.1 | 2.5 | 83.7 | — | — |
| | $Sn_4AuNi_2$/$Sn_4Au$/$SnNi_3$ | 28.2 | 13.3 | 11.5 | 8.2 | 41.4 | 0.3 |
| | $SnNi_3$/$Sn_2Au$/$SnAu$ | 20.6 | 26.2 | 0.2 | 32.1 | 4.5 | 44.4 |
| | $Sn_2Ni_3$/hcp/$SnAu$ | 22.7 | 29.1 | 0.2 | 84.5 | 0.8 | 48.2 |

the Sn-Au-Ni system are listed in Table IV. In the present work, the Gibbs energy of the $Sn_2Ni_3$ phase is described by the three-sublattice model, as shown in the previous section.

As discussed above, the crystal structures of the $Sn_2Ni_3$ and SnAu phases are, respectively, the $Ni_2In$- and NiAs-type structures. Thus, the Gibbs energies of the $Sn_2Ni_3$ phase with the solubility of

Au and the SnAu phase with the solubility of Ni are described by a different model.

On the basis of the present experimental data in the Sn-Au-Ni system, the ternary thermodynamic parameters of the liquid, hcp, $Sn_2Ni_3$, $Sn_4Au$, and SnAu phases, as well as the $Sn_4AuNi_2$ ternary compound, were assessed, and the calculated isothermal sections with the experimental data are shown
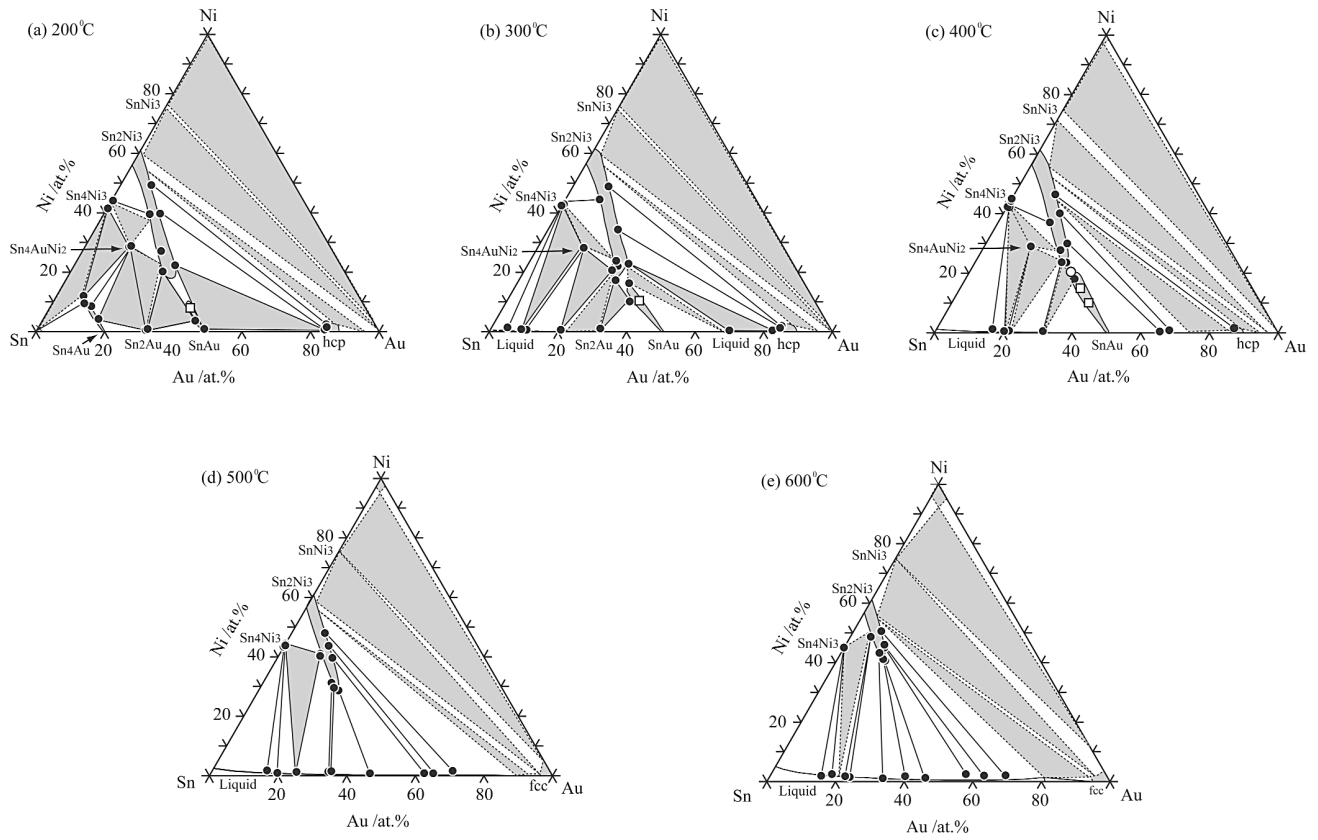
Fig. 3. Isothermal sections at (a) 200°C, (b) 300°C, (c) 400°C, (d) 500°C, and (e) 600°C determined by the present work. ●: Phase equilibria, ○: Two-phase alloy, □: Single-phase alloy.
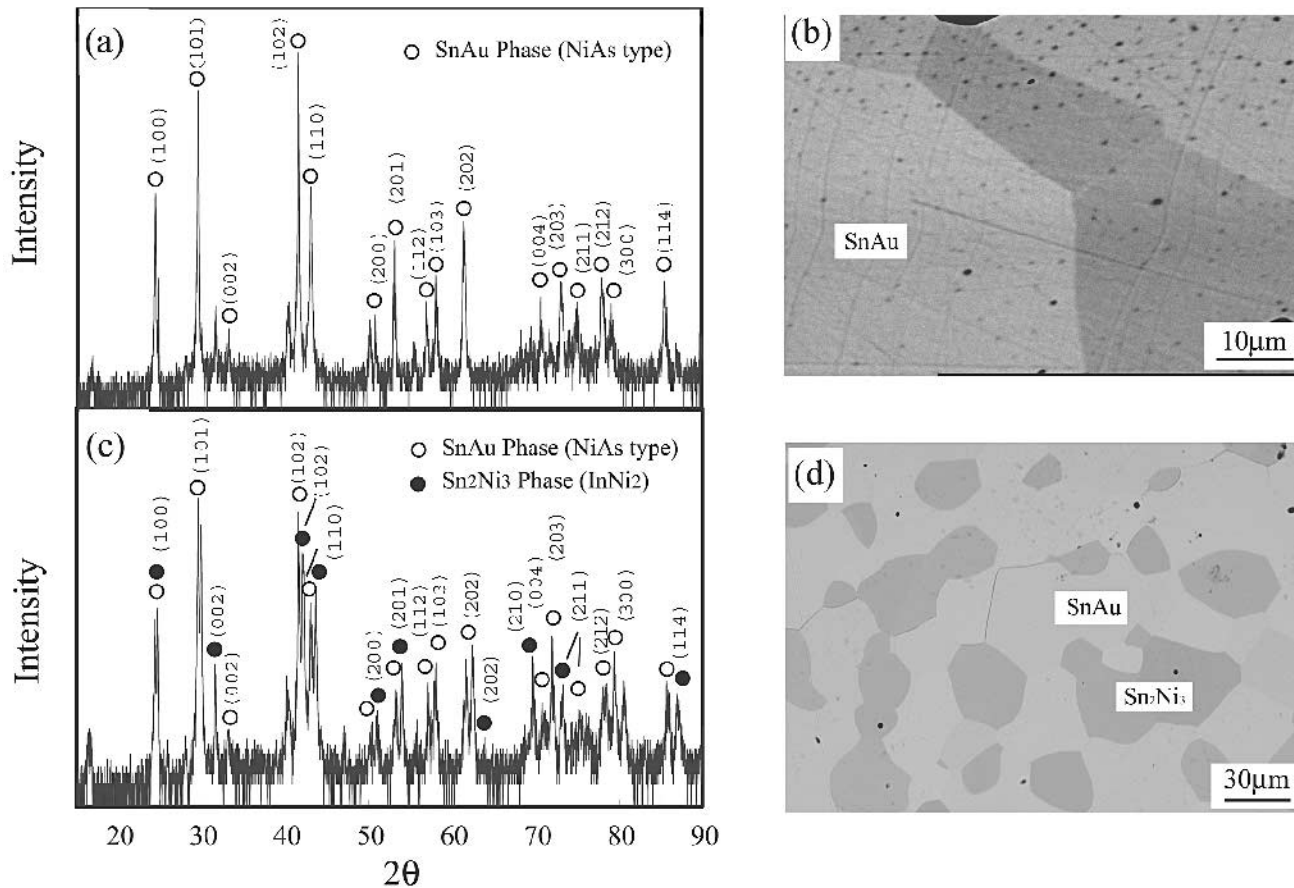


Fig. 4. X-ray diffraction patterns and microstructure of the (a) and (b) SnAu$_5$Ni$_{15}$ and (c) and (d) SnAu$_{30}$Ni$_{20}$ alloys equilibrated at 400°C for 40 days.

**Table III. Transformation Temperatures Determined by Differential Scanning Calorimetry**

| Alloy Composition (At.%) | | Liquidus (°C) | Other Transformation Temperature (°C) |
|---|---|---|---|
| **Ni** | **Au** | | |
| 25 | 25 | 1017 | 311, 518 |
| 17.5 | 17.5 | 880 | 260, 408 |
| 12.5 | 12.5 | 775 | 211, 240, 316, 711 |
| 5 | 5 | 605 | 216, 241 |
| 40 | 10 | 1168 | 513, 484 |
| 10 | 40 | 865 | 315, 445 |
| 45 | 15 | 1150 | 402 |
| 30 | 30 | 1030 | 284, 304 |
| 15 | 45 | 875 | 280, 335 |
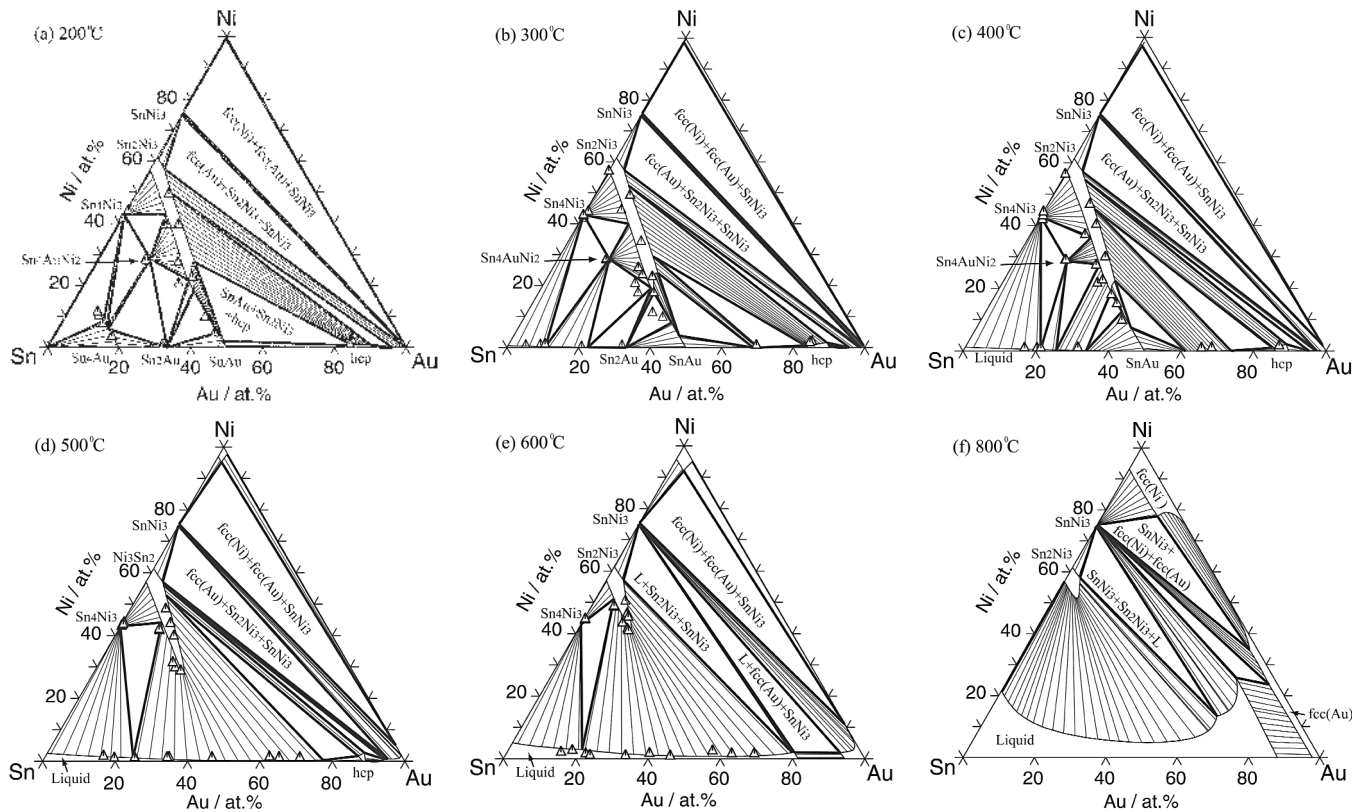


Fig. 5. Calculated isothermal sections at (a) 200°C, (b) 300°C, (c) 400°C, (d) 500°C, (e) 600°C, and (f) 800°C compared with the present experimental data.

in Fig. 5a through e. It is seen that there is good agreement between the calculated results and experimental data. The calculated isothermal section at 800°C is also presented in Fig. 5f. Very satisfactory agreement between the calculated vertical sections and the experimental data is shown in Fig. 6. Figure 6d shows the calculated vertical section including the $Sn_4AuNi_2$ ternary compound. It is seen that the ternary compound is stable until 422°C, at which a peritectic reaction occurs. The calculated results are in good agreement with the experimental results. Based on the optimized thermodynamic parameters, the calculated liquidus projection of this system is shown in Fig. 7, in which there are one eutectic, two peritectic, and ten quasi-peritectic

reactions. The invariant reactions are summarized in Table V.

## CONCLUSIONS

- The phase equilibria of the Sn-Au-Ni system, including six isothermal sections and three vertical sections, were determined. The characteristics of the phase equilibria in this system are as follows: (a) there is a ternary compound ($Sn_4AuNi_2$) in the Sn-rich portion; (b) there is a larger solubility of Ni in the $Sn_4Au$ phase in the Sn-Au system; and (c) there is a phase equilibrium between the $Sn_2Ni_3$ and the SnAu phases, rather than the extended homogeneity solution reported previously.

## Table IV. Thermodynamic Parameters in the Ternary Sn-Au-Ni System Used in This Work (J/mol)

**Liquid Phase (Au,Ni,Sn)**

$^0L_{Au,Ni}^{liq} = -40,014.59 - 30.286*T$

$^1L_{Au,Ni}^{liq} = -822.33 - 0.536*T$

$^0L_{Au,Sn}^{liq} = -48,822.94 + 19.68*T - 2.84*T*Ln(T)$

$^1L_{Au,Sn}^{liq} = -17,990.36 + 0.79*T$

$^2L_{Au,Sn}^{liq} = -5,222.53$

$^0L_{Ni,Sn}^{liq} = -140,308.48 + 386.9*T - 44.67*T*Ln(T)$

$^1L_{Ni,Sn}^{liq} = -60,955.58 + 155.55*T - 18.82*T*Ln(T)$

$^0L_{Au,Ni,Sn}^{liq} = -20,000$

**Fcc Phase (Au,Ni,Sn)**

$^0L_{Au,Ni}^{fcc} = 38,588.32 - 20.21*T$

$^1L_{Au,Ni}^{fcc} = -563.43 - 2.84*T$

$^0L_{Au,Sn}^{fcc} = -28,802.84 - 5.58*T$

$^1L_{Au,Sn}^{fcc} = 8,515.07 - 11.79*T$

$^0L_{Ni,Sn}^{fcc} = -60,397.19 + 5.97*T$

$^1L_{Ni,Sn}^{fcc} = -25,786.96 + 4.92*T$

**Sn$_4$AuNi$_2$ Compound (Sn)$_{0.571}$ (Au)$_{0.143}$(Ni)$_{0.286}$**

$G_{Au:Ni:Sn}^{AuNi_2Sn_4} - 0.571° G_{Sn}^{bct} - 0.143° G_{Au}^{fcc} - 0.286° G_{Ni}^{fcc} = -22,795.79 + 2.633*T$

**Sn$_2$Ni$_3$ Phase (Ni,Sn)$_{0.5}$(Au,Ni)$_{0.25}$(Au,Ni)$_{0.25}$**

$G_{Ni:Ni:Ni}^{Sn_2Ni_3} - ° G_{Ni}^{hcp} = 0.0$

$G_{Ni:Au:Au}^{Sn_2Ni_3} - 0.5° G_{Ni}^{fcc} - 0.5° G_{Au}^{fcc} = -1365 + 5*T$

$G_{Ni:Au:Ni}^{Sn_2Ni_3} - 0.75° G_{Ni}^{fcc} - 0.25° G_{Au}^{fcc} = °G_{Ni:Ni:Au}^{Sn_2Ni_3} - 0.75° G_{Ni}^{fcc} - 0.25° G_{Au}^{fcc} = 1,000$

$G_{Sn:Au:Au}^{Sn_2Ni_3} - 0.5° G_{Ni}^{fcc} - 0.5° G_{Au}^{fcc} = -12,976.31 + 1.02*T$

$G_{Sn:Ni:Ni}^{Sn_2Ni_3} - 0.5° G_{Sn}^{bct} - 0.5° G_{Ni}^{fcc} = -22,103.5 + 1.828*T$

$G_{Sn:Au:Ni}^{Sn_2Ni_3} - 0.5° G_{Sn}^{bct} - 0.25° G_{Au}^{fcc} - 0.25° G_{Ni}^{fcc} = G_{Sn:Ni:Au}^{Sn_2Ni_3} - 0.5° G_{Sn}^{bct} - 0.25° G_{Au}^{fcc} - 0.25° G_{Ni}^{fcc} = -19,289.91 + 1.42435*T$

$^0L_{Sn:Au:Au, Ni}^{Sn_2Ni_3} = -6,000$

$^1L_{Sn:Au:Au, Ni}^{Sn_2Ni_3} = -500$

$^0L_{Sn:Ni:Au, Ni}^{Sn_2Ni_3} = -19,460 + 20*T$

$^0L_{Sn:Au, Ni:Au}^{Sn_2Ni_3} = 0$

$^1L_{Sn:Au, Ni:Au}^{Sn_2Ni_3} = -500$

$^0L_{Sn:Au, Ni:Ni}^{Sn_2Ni_3} = -6,000$

$^0L_{Ni,Sn:Au:Au}^{Sn_2Ni_3} = -20,000$

$^0L_{Ni,Sn:Au:Ni}^{Sn_2Ni_3} = {}^0L_{Ni,Sn:Ni:Au}^{Sn_2Ni_3} = -10,000$

$^0L_{Ni,Sn:Ni:Ni}^{Sn_2Ni_3} = -35,773.7 + 20.124*T$

$^1L_{Ni,Sn:Ni:Ni}^{Sn_2Ni_3} = 86,534.3$

**Sn$_2$Au Compound (Sn)$_{0.667}$(Au)$_{0.333}$**

$G_{Sn:Au}^{Sn_2Au} - 0.667° G_{Sn}^{bct} - 0.333° G_{Au}^{fcc} = -17,419.12 + 10.905*T$

**Sn$_4$Au Compound (Sn)$_{0.8}$(Au,Ni)$_{0.2}$**

$G_{Sn:Au}^{AuSn_4} - 0.8° G_{Sn}^{bct} - 0.2° G_{Au}^{fcc} = -9,770.27 + 4.4335*T$

$G_{Sn:Ni}^{Sn_2Au} - 0.8° G_{Sn}^{bct} - 0.2° G_{Ni}^{fcc} = -15,825 + 25*T$

$^0L_{Sn:Ni,Au}^{Sn_2Au} = -43,650 + 50*T$

**SnAu$_5$ Compound (Sn)$_{0.16}$(Au)$_{0.84}$**

$G_{Sn:Au}^{SnAu_5} - 0.16° G_{Sn}^{bct} - 0.84° G_{Au}^{fcc} = -4,050 - 3.3*T$

**SnAu$_{10}$ Phase (Au,Sn)**

$G_{Au}^{SnAu_{10}} - ° G_{Au}^{fcc} = 125 + 0.79*T$

$G_{Sn}^{SnAu_{10}} - ° G_{Sn}^{bct} = 3,804 - 3.46*T$

$^0L_{Au,Sn}^{SnAu_{10}} = -13,427.03 - 5.2576*T$

$^1L_{Au,Sn}^{SnAu_{10}} = -14,823.13 - 21.1189*T$

**Bcc Phase (Au,Ni,Sn)**

$G_{Au}^{bcc} - ° G_{Au}^{fcc} = 4,250 - 1.1*T$

$G_{Ni}^{bcc} - ° G_{Ni}^{fcc} = 8,715.08 - 3.556*T$

$G_{Sn}^{bcc} - ° G_{Sn}^{bct} = 4,400 - 6*T$

$^0L_{Au,Ni}^{bcc} = 50*T$

$^0L_{Au,Ni}^{bcc} = 30,000$

$^0L_{Ni,Sn}^{bcc} = 0.0$

$^0L_{Au,Sn}^{bcc} = 0.0$

$^0L_{Au,Ni,Sn}^{bcc} = 0.0$

**βSn Phase (Ni,Sn)**

$G_{Ni}^{βSn} - ° G_{Sn}^{bct} = 10,023 - 4.556*T$

$G_{Sn}^{βSn} - ° G_{Sn}^{bct} = 0.0$

$^0L_{Ni,Sn}^{βSn} = -21,500$

**Hcp Phase (Au,Ni,Sn)**

$G_{Au}^{hcp} - ° G_{Au}^{fcc} = 241.75 + 1.6*T$

$G_{Ni}^{hcp} - ° G_{Ni}^{fcc} = 6,610.72$

$G_{Sn}^{hcp} - ° G_{Sn}^{bct} = 3,900 - 4.4*T$

$^0L_{Au,Ni}^{hcp} = 4,500$

$^0L_{Ni,Sn}^{hcp} = 2,000$

$^0L_{Au,Sn}^{hcp} = -13,145.27 - 6.4932*T$

$^1L_{Au,Sn}^{hcp} = -19,184.81 - 25.1676*T$

$^0L_{Au,Ni,Sn}^{hcp} = -506,500 + 500*T$

**SnAu Compound (Sn)$_{0.5}$(Au,Ni)$_{0.5}$**

$G_{Sn:Au}^{SnAu} - 0.5° G_{Sn}^{bct} - 0.5° G_{Au}^{fcc} = -29,952.62 + 2.0412*T$

$G_{Sn:Ni}^{SnAu} - 0.5° G_{Sn}^{bct} - 0.5° G_{Ni}^{fcc} = -50,000$

**Sn$_4$Ni$_3$ Compound (Ni,Sn)$_{0.5714}$(Ni)$_{0.4286}$**

$G_{Ni:Ni}^{Sn_4Ni_3} - ° G_{Ni}^{fcc} = 5,000$

$G_{Sn:Ni}^{Sn_4Ni_3} - 0.5714° G_{Sn}^{bct} - 0.4286° G_{Ni}^{fcc} = -25,180.39 + 2.1289*T$

$^0L_{Ni,Sn:Ni}^{Sn_4Ni_3} = -11,991.46$

$^1L_{Ni,Sn:Ni}^{Sn_4Ni_3} = 9,991.44$

**SnNi$_3$-HT Compound (Ni,Sn)$_{0.25}$(Ni,Sn)$_{0.75}$**

$G_{Ni:Ni}^{SnNi_3 -HT} - ° G_{Ni}^{fcc} = 8,715.08 - 3.556*T$

$G_{Ni:Sn}^{SnNi_3 -HT} - 0.25° G_{Ni}^{fcc} - 0.75° G_{Sn}^{bct} = 39,653.24 - 13.6541*T$

$G_{Sn:Ni}^{SnNi_3 -HT} - 0.25° G_{Sn}^{bct} - 0.75° G_{Ni}^{fcc} = -26,538.16 - 4.0981*T$

$G_{Sn:Sn}^{SnNi_3 -HT} - ° G_{Sn}^{bct} = 4400 - 6*T$

$^0L_{Ni:Ni,Sn}^{SnNi_3 -HT} = {}^0L_{Sn:Ni,Sn}^{SnNi_3 -HT} = -20,649.75 + 4.2325*T$

$^0L_{Ni,Sn:Ni}^{SnNi_3 -HT} = {}^0L_{Ni,Sn:Sn}^{SnNi_3 -HT} = 18,404.58 - 11.8855*T$

**SnNi$_3$-LT Compound (Ni,Sn)$_{0.25}$(Ni,Sn)$_{0.75}$**

$G_{Ni:Ni}^{SnNi_3 -LT} - ° G_{Ni}^{fcc} = 1,046 + 1.255*T$

$G_{Ni:Sn}^{SnNi_3 -LT} - 0.25° G_{Ni}^{fcc} - 0.75° G_{Sn}^{bct} = -21,711.47 - 7.3299*T$

$G_{Sn:Ni}^{SnNi_3 -LT} - 0.25° G_{Sn}^{bct} - 0.75° G_{Ni}^{fcc} = -26,657.47 + 4.1849*T$

$G_{Sn:Sn}^{SnNi_3 -LT} - ° G_{Sn}^{bct} = 3,900 - 4.4*T$

$^0L_{Ni:Ni,Sn}^{SnNi_3 -LT} = {}^0L_{Sn:Ni,Sn}^{SnNi_3 -LT} = -20,578.9 = 5 + 5.2632*T$

$^0L_{Ni,Sn:Ni}^{SnNi_3 -LT} = {}^0L_{Ni,Sn:Sn}^{SnNi_3 -LT} = -1,510.59 + 7.3684*T$
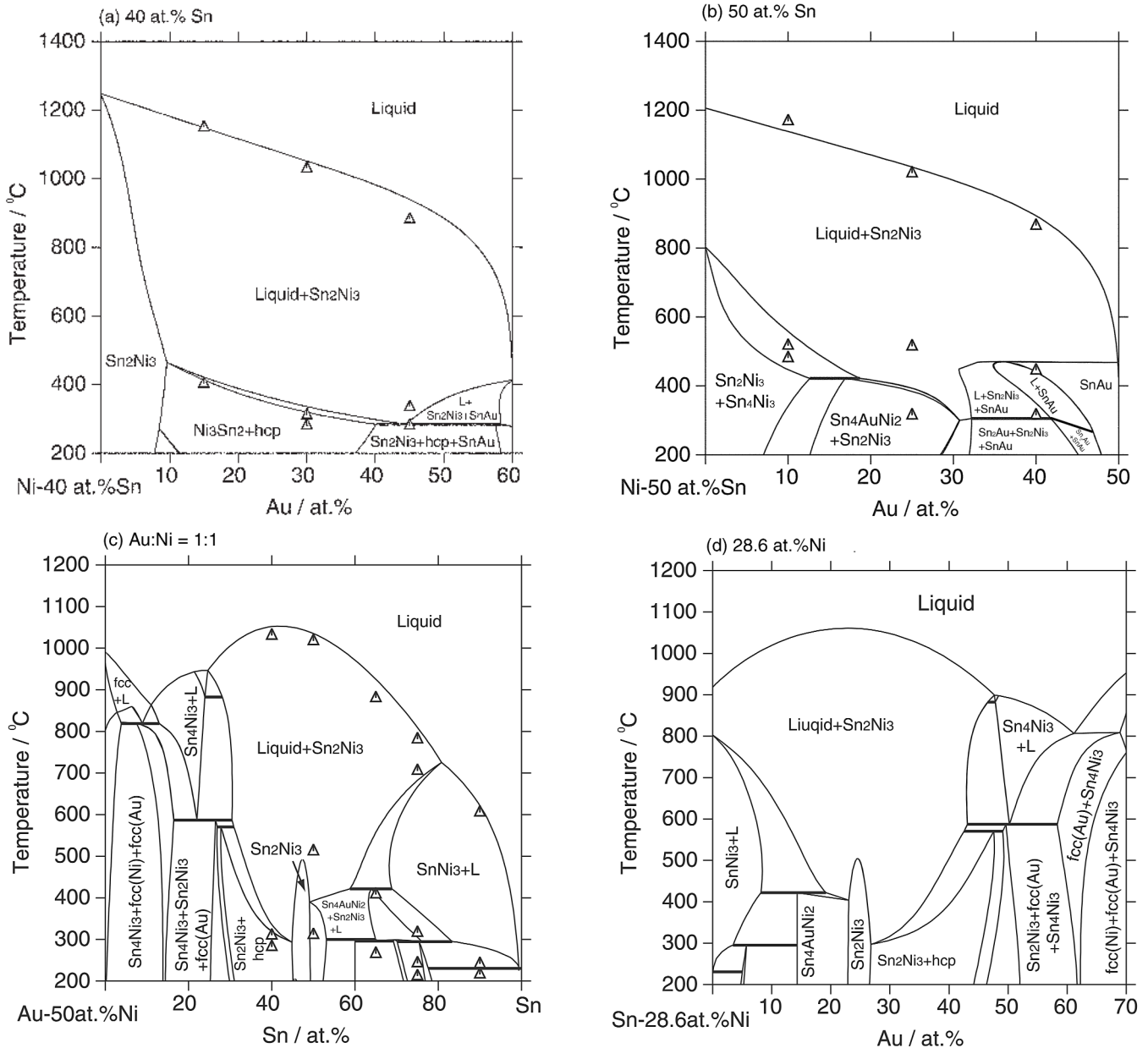
Fig. 6. Calculated vertical sections at (a) 40at.%Sn, (b) 50at.%Sn, (c) Au:Ni = 1:1, and (d) 28.6at.%Ni compared with the present experimental data.

- Thermodynamic assessment of the Sn-Au-Ni system was carried out on the basis of the CALPHAD method. The thermodynamic parameters for describing the phase equilibria were optimized, resulting in good agreement between calculated and experimental data.

## ACKNOWLEDGEMENTS

## REFERENCES

1. A.M. Minor and J.W. Morris, *J. Electron. Mater.* 29, 1170 (2000).
2. C.E. Ho, R. Zheng, G.L. Luo, A.H. Lin, and C.R. Kao, *J. Electron. Mater.* 29, 1175 (2000).
3. H.G. Song, J.P. Ahn, A.M. Minor, and J.W. Morris, *J. Electron. Mater.* 30, 409 (2001).
4. C.E. Ho, L.C. Shiau, and C.R. Kao, *J. Electron. Mater.* 31, 1264 (2002).
5. A. Neumann, A. Kjekshus, and E. Rost, *J. Solid State Chem.* 123, 203 (1996).
6. S. Anhock, H. Oppermann, C. Kallmayer, R. Aschenbrenner, L. Thomas, and H. Reichl, *Proc. 22th IEEE/CPMT Int. Electron. Manufacturing Technol. Symp.* (New York: IEEE, 1998), pp. 156–165.
7. N. Saunders and A.P. Miodownik, *CALPHAD* (Oxford, U.K.: Pergamon, 1998).

**Table V. Calculated Invariant Reactions of the Sn-Au-Ni System**

| Reaction | Temperature (°C) | Liquid Composition (At.%) | |
|---|---|---|---|
| | | Au | Ni |
| $L \Leftrightarrow Sn_4Ni_3 + Sn_4Au + \beta Sn$ (E) | 230.2 | 0.23 | 0.33 |
| $L + Sn_2Ni_3 \Leftrightarrow SnAu + hcp$ (P1) | 284.4 | 69.7 | 0.002 |
| $L + Sn_4AuNi_2 \Leftrightarrow Sn_4Ni_3 + Sn_4Au$ (P2) | 295.2 | 10.3 | 0.31 |
| $L + Sn_4AuNi_2 \Leftrightarrow Sn_4Au + Sn_2Au$ (P3) | 296.5 | 21.4 | 0.08 |
| $L + Sn_2Ni_3 \Leftrightarrow Sn_4AuNi_2 + Sn_2Au$ (P4) | 299.9 | 22.6 | 0.08 |
| $L + SnAu \Leftrightarrow Sn_2Au + Sn_2Ni_3$ (P5) | 304.9 | 24.6 | 0.06 |
| $L + Sn_2Ni_3 + Sn_4Ni_3 \Leftrightarrow Sn_4AuNi_2$ (P6) | 421.7 | 24.2 | 0.54 |
| $L + Sn_2Ni_3 \Leftrightarrow Sn_4Ni_3 + SnAu$ (P7) | 445.3 | 25.7 | 0.64 |
| $L + fcc \Leftrightarrow hcp + SnAu_{10}$ (P8) | 529.4 | 79.3 | 0.05 |
| $L + Sn_2Ni_3 + fcc \Leftrightarrow hcp$ (P9) | 570.2 | 79.3 | 1.3 |
| $L + SnNi_3\text{-LT} \Leftrightarrow Sn_2Ni_3 + fcc$ (P10) | 587.1 | 79.4 | 1.7 |
| $L + SnNi_3\text{-HT} \Leftrightarrow SnNi_3\text{-LT} + Sn_2Ni_3$ (P11) | 882.2 | 51.1 | 25.5 |
| $L + Ni_3Sn\text{-HT} \Leftrightarrow Ni_3Sn\text{-LT} + fcc$ (P12) | 937.0 | 27.9 | 59.0 |
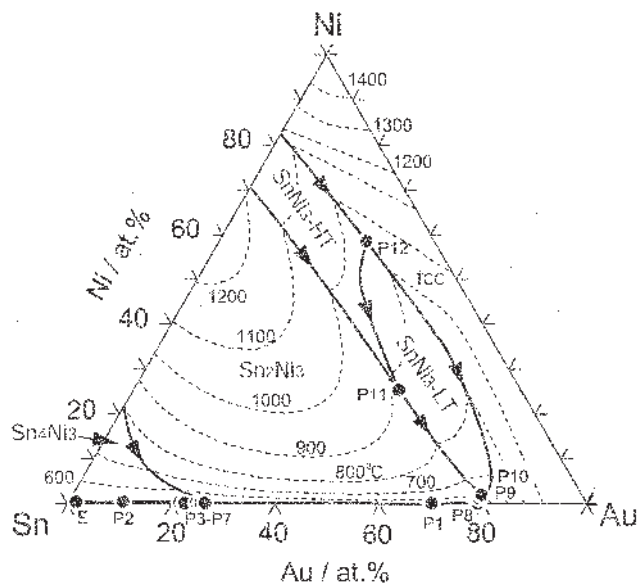


Fig. 7. Calculated liquidus projection in the Sn-Au-Ni ternary system.

8.  I. Ohnuma, X.J. Liu, H. Ohtani, and K. Ishida, *J. Electron. Mater.* 28, 1163 (1999).
9.  X.J. Liu, I. Ohnuma, C.P. Wang, M. Jiang, R. Kainima, K. Ishida, M. Ode, T. Koyama, H. Onodera, and T. Suzuki, *J. Electron. Mater.* 32, 1265 (2003).
10. X.J. Liu, K. Oikawa, I. Ohnuma, R. Kainuma, and K. Ishida, *JOM* 55, 53 (2003).
11. J.-P. Jan, W.B. Pearson, A. Kjekshus, and S.B. Woods, *Can. J. Phys.* 41, 2252 (1963).
12. K. Schubert, H. Breimer, and R. Gohle, *Z. Metallkd.* 50, 146 (1959).
13. R. Kubiak and M. Wolcyrz, *J. Less-Common Met.* 97, 265 (1984).
14. K. Osada, S. Yamaguchi, and M. Hirabayashi, *Trans. Jpn. Inst. Met.* 15, 256 (1974).
15. K. Schubert, W. Burkhardt, P. Esslinger, E. Günzel, H.G. Meissner, W. Schütt, J. Wegst, and M. Wilkens, *Naturwissenschaften* 43, 248 (1956).
16. F. Lihl and H. Kirnbauer, *Monatsh. Chem.* 86, 745 (1955).
17. H. Fjellvag and A. Kjekshus, *Acta Chem. Scand.* 40A, 23 (1986).
18. H. Fjellvag and A. Kjekshus, *Acta Chem. Scand.* 40A, 695 (1986).
19. A. Neumann, A. Kjekshus, C. Romming, and E. Rost, *J. Solid State Chem.* 119, 142 (1995).
20. O. Redlich and A.T. Kister, *Ind. Eng. Chem.* 40, 345 (1948).
21. M. Hillert and L.I. Staffansson, *Acta Chem. Scand.* 24, 3618 (1970)
22.  A.T. Dinsdale, *CALPHAD* 15, 317 (1991).
23. G. Ghosh, *Metall. Mater. Trans. A* 30A, 1481 (1999).
24. H.S. Liu, C.L. Liu, K. Ishida, and Z.P. Jin, *J. Electron. Mater.* 32, 1290 (2003).
25. S. Morioka and M. Hasebe, *J. Phase Equilibrium* 20, 244 (1999).